Chin. J. Astron. Astrophys. Vol. 1, No. 4, (2001) 296–304
(http://www.chjaa.org or http://chjaa.bao.ac.cn)

Chinese Journal of
Astronomy and
Astrophysics

Spectral Reversal and Stratification of the Jet in 3C 273

Shan-Jie Qian[1,2] ⋆, Xi-Zheng Zhang[1], T. P. Krichbaum[2], A. Kraus[2], A. Witzel[2] and J. A. Zensus[2]

[1] National Astronomical Observatories, Chinese Academy of Sciences, Beijing 100012
[2] Max-Planck-Institut für Radioastronomie, Auf dem Hügel 69, D-53121 Bonn, Germany

Received 2000 December 15; accepted 2001 June 23

Abstract Quasi-simultaneous VLBI observations at 15–86 GHz have shown that in the classical superluminal radio source 3C 273, the spectral index α ($S_\nu \propto \nu^\alpha$) has a systematic variation along the jet. For epoch 1995.15, a spectral reversal was observed at core distance ~ 1.5 mas, where the superluminal knot C12 located. Similarly, for epoch 1997.18, two spectral reversals were observed at core distances of $\sim$1.8 mas and $\sim$4.2 mas, where superluminal knots C11 and C14 were, respectively. These spectral reversals are associated with local maxima of the jet width. We suggest that this phenomenon may be related to a stratification of the jet structure, i.e., its physical parameters (flow velocity, Doppler factor, electron density and energy, magnetic field strength, etc.) are substantially dependent on the distance from the jet axis. These properties may be naturally formed through gasdynamic processes when the jet expands into a lower pressure ambient medium.

Key words: galaxies: active – galaxies: compact – quasars: individual: 3C 273 – galaxies: jets – radio continuum: galaxies – radiation mechanisms: non-thermal

1 INTRODUCTION

The quasar 3C 273 ($z = 0.158$) is a well known classical superluminal radio source (Zensus 1997). It reveals strong variability in all wavebands from radio, IR/optical, X-ray to γ-ray and has been studied intensively (Babadzhanyants & Belokon 1992; Courvoisier 1998; Stevens et al. 1998; Türler et al. 1999a; 1999b; Von Montigny et al. 1997; Pauliny et al. 1987; Qian et al. 1999a, 1999b). Superluminal knots are intermittently ejected and separated from the VLBI-core (Cohen et al. 1987; Zensus et al. 1990; Bååth et al. 1991; Abraham et al. 1996; Krichbaum et al. 1992; 1998b). A relationship between the high energy activity in optical-X ray-γ ray bands and the ejection of superluminal knots has been established.

3C 273 has been observed with VLBI for more than thirty years. It is found that superluminal knots in 3C 273 move basically along straight lines (core distance >0.5 mas), but different knots are observed to have different apparent velocities and different position angles. On the

⋆ E-mail: rqsj@class1.bao.ac.cn

basis of cm-VLBI observations Abraham & Romero (1999) found that the position angle (PA) of the superluminal knots, ejected successively from the core, has a periodic variation with a period of ∼16 years in the observer's frame. They suggested that the PA rotation is due to the precession of the jet. They assumed that the jet precesses and sweeps a cone with a half opening angle of ∼ 5.4°. Their model can well fit the periodic PA rotation of the knots C2–C9. But they suggested that these superluminal knots are ejected from the core with the same velocity (Lorentz factor). Therefore the difference observed in the apparent velocity of the knots is ascribed to the variation of the viewing angle, caused by the precession of the jet.

In recent years mm-VLBI observations have been carried out for strong variable sources. Due to having higher resolutions than at cm wavelengths, the mm-VLBI observations are very useful for early detection of the ejection of superluminal knots and identification of the correlation between optical outbursts and the formation of superluminal knots. A good example is the large optical/IR outburst which was observed to be followed by a superluminal component C9 (Krichbaum et al. 1990; Bååth et al. 1991; Courvoisier et al. 1988; Courvoisier 1998). Most recently, the 43–86 GHz VLBI observations (with the highest resolution of ∼50μas) made by Krichbaum et al. (2001) during the period 1992–1997 provides new information about the structure of the 3C 273 jet and the kinematics of the knots (<5 mas). For example, they found that for each individual knot (C9–C17) the apparent velocity increases outwards and the jet observed at mm wavelengths reveals curvatures on submas scales. They also found some new phenomena, which can be summarized as follows.

- The periodic variation of the ejection direction of the superluminal knots, i.e., the rotation of the position angle of the successive knots is confirmed, but with a period of ∼15 years.
- The variation of the apparent velocity of the knots during the period 1963–1997 is not periodic as expected from the model of Abraham & Romero (1999). The apparent velocity systematically decreases at a rate $\mathrm{d}\beta_{\mathrm{app}}/\mathrm{dt}\sim$–0.16 mas yr^{-1}, on which a short-period oscillation is superimposed. For example, the apparent velocity of C9 (ejected at 1988.0) is 6.2c, while for C15 (ejected at 1995.4) it is only 3.1c.
- the jet observed at 86 GHz is narrower (or more compact) than observed at lower frequencies (15–22 GHz). The 86 GHz radiation is much closer to the jet axis, showing a different transverse distribution at different frequencies (or some sort of stratification across the jet).
- The ridge of the jet and the jet width are found to be oscillating with a wavelength of ∼1.5–2 mas, i.e., the jet reveals systematic expansion and recollimation.
- From quasi-simultaneous VLBI observations at 15–86 GHz at two epochs (1995.15 and 1997.18), it is found that the variation of the spectral index (α(15–86 GHz)) along the jet is also oscillating.
- The variation of the spectral index is associated with the variation of the jet width, i.e., the maximal spectral index corresponds to the local maximal jet width.

Qian et al. (2001) have proposed a new precessing jet model to explain the kinematic behavior of the superluminal knots. In the model both the jet precession and the variation of the ejection Lorentz factor with time are taken into account, and the association of the VLBI behavior (periodicities) with a binary black hole system is discussed. In this paper we will concentrate on a discussion of the spectral index distribution along the jet and its implications. Throughout the paper a Hubble constant $H_0 = 100\,\mathrm{km\,s^{-1}\,Mpc^{-1}}$ and a deceleration parameter

$q_0 = 0.5$ are used. Thus the angular scale of 1 mas corresponds to a spatial scale of 1.78 pc for 3C 273 and an angular speed of 1 mas yr^{-1} corresponds to an apparent velocity of $\beta_{\rm app}$=6.8.

2 SPECTRAL REVERSAL: PHENOMENON

As described above, quasi-simultaneous VLBI observations at 15–86 GHz have shown systematic variations of the spectral index along the jet. The phenomenon can be read from Fig. 1, which displays the spectral index α (22–86 GHz) distribution along the jet for epoch 1995.15. This distribution was derived from the superluminal knots, which were model-fit by Gaussian components at 22 and 86 GHz. It can be seen, at zero distance (or at the VLBI core) the spectrum is inverted with $\alpha \sim 1.3$. Within core distance of ~ 0.5 mas (where knot C13a is), the spectrum steepens and gradually becomes negative. But between $\sim$0.5 mas and $\sim$1.5 mas (knot C12), the spectrum flattens and gradually becomes inverted with α>0. Then beyond $\sim$1.5 mas the spectrum steepens again and α reaches a minimum at $\sim$2.5 mas, location of knot C11.

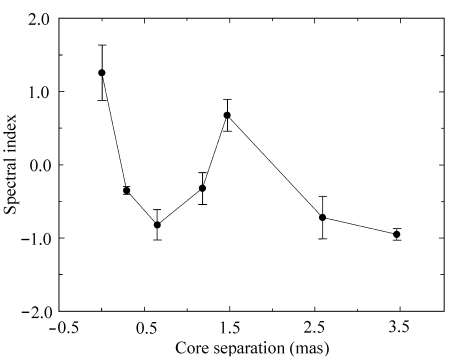

Fig. 1 Distribution of the spectral index ($S_\nu \propto \nu^\alpha$) along the jet revealed by the superluminal knots for epoch 1995.15. It shows a spectral reversal (or inversion) at core distance $\sim$1.5 mas. In order of core distance the filled points are for the VLBI core and knots C14, C13a, C13b, C12, C11 and C10.

Interestingly, such an oscillating distribution of the spectral index was detected once again at epoch 1997.18. Using the intensity profiles of the jet at 15 and 86 GHz, Krichbaum et al. (2001) obtained the spectral index distribution along the jet. It can be seen (see fig. 16 in Krichbaum et al. 2001) that at core distances $\sim$1.8 mas and $\sim$4.2 mas the spectral index reaches maxima (i.e., the spectrum is inverted with α>0). We point out that now at core distance $\sim$1.8 mas, there is a new knot, C14. Together with the inverted spectrum of C12 at core distance $\sim$1.5 mas for epoch 1995.15, we come to the conclusion that the spectral inversion only depends on the specific position (maximal expansion) along the jet. It does not depend on which knot occupies this position at the time. In other words, during the period 1995.15 –1997.18 the jet region (core distance less than $\sim$3 mas) is stable, although different superluminal knots move through this region.

Figure 2 shows the variation of the flux density of the knot C12a observed at 15, 22, 43 and 86 GHz during the period 1993.0–1997.3. It is clearly seen that during 1992.8–1993.5 the 22 GHz flux density was much higher than the 43 GHz flux density, but at epoch 1995.15 the 86 GHz flux density is much higher than the 22 GHz flux density. And after ∼1996.0 the 86 GHz flux density again decreases below the 15 GHz flux density. So Fig. 2 clearly shows the spectral evolution of knot C12a. It can be seen that the spectral reversal (or inversion) of knot C12a at epoch 1995.15 is mainly due to the dramatic increase of its 86 GHz flux density.

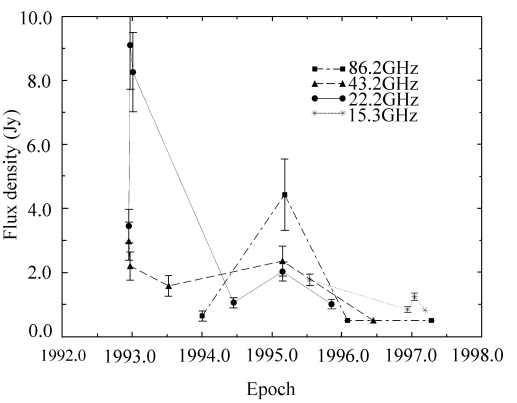

Fig. 2 Variations of the flux density of knot C12a observed at 15, 22, 43 and 86 GHz. The three data points without error bars are upper limits.

We point out that the phenomenon observed in the jet of 3C 273 has also been observed in the FRII radio galaxy Cygnus-A. On the basis of the VLBI observations at 22 and 43 GHz, Krichbaum et al. (1998a) found that on submas and mas scales the transverse width of the jet oscillates systematically and the spectrum flattens significantly at core distance of ∼1–2 mas. This spectral flattening is related to a local maximum of the transverse width of the jet. Moreover in the case of Cygnus-A, an apparent acceleration from $\sim 0.1 - 0.2c$ (at ∼1–2 mas) to $\sim 0.7c$ (at ∼15 mas) was observed. The transition from slow to fast motion occurs at ∼1 mas. From the new findings for both 3C 273 and Cygnus-A, we recognize that the correlation between the spectral flattening, jet width oscillation and apparent flow acceleration may be important for understanding the physical processes occurring in relativistic jets. This phenomenon could be related to intrinsic changes of superluminal knots (electron acceleration and field magnification etc.) and changes of Doppler beaming (bulk acceleration or change of viewing angle). Although helical motion of superluminal knots or jet flow (lighthouse effect and KH instabilities) could be involved (Qian et al. 1991, 1996; Camenzind & Kronkenburger 1992; Hardee 1995), the tight correlation between the spectral reversal and the expansion of the jet in two sources (3C 273 and Cygnus-A) seems to be in favor of gasdynamic properties of relativistic jets (Daly & Marscher 1988). We will show below that this phenomenon is a natural consequence of the hydrodynamic behavior of relativistic jets.

3 GASDYNAMIC PROPERTIES OF RELATIVISTIC JETS

We apply the gasdynamical model proposed by Daly & Marscher (1988) for expanding relativistic jets to explain the observed spectral reversal and its correlation with the oscillation of the jet width. We also estimate some of the parameters of the emitting regions which are consistent with the VLBI measurements.

In the gasdynamic model, Daly & Marscher used the method of characteristics to study the flow properties of a relativistic jet, which consists of relativistic particles and a dynamically weak, frozen-in magnetic field and which expands into a region of uniform lower pressure. Let the jet enter the external medium along the z-axis, with an initial Lorentz factor Γ_0 and pressure P_0 (Fig. 3). Let the initial radius of the jet be r_0 and the pressure of the external uniform medium be P_e. From the theoretical calculations (Daly & Marscher 1988), it is found that the properties of the jet (the shape of the jet boundary, the flow velocity, pressure and the internal energy density, etc.) only depend on two parameters: the initial Lorentz factor Γ_0 and the ratio of the external pressure to the initial pressure of the gas in the jet, R_p=P_e/P_0.

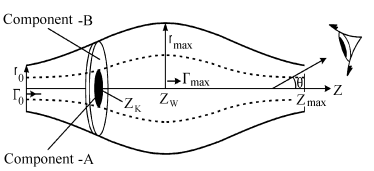

Fig. 3 A sketch of the stratified jet model based on gasdynamic behavior of expanding relativistic jets (not to scale).

In the case of the jet encountering a mild pressure drop ($0.5 \lesssim R_p \lesssim 1$), the jet first expands into the region of lower pressure and then contracts, resulting in an oscillating pattern of the jet cross section. This is due to the repeated decollimation and recollimation of the jet flow. The maximum width of the jet is given by:

$$r_{\max} \approx r_0[1 + 1.9(1 - {R_p}^{1/4})/(2{R_p}^{1/4} - 1)]\,. \tag{1}$$

The wavelength of the oscillation (or the characteristic length) is given by:

$$z_{\max} \approx 5.5 r_0 \Gamma_0/(2{R_p}^{1/4} - 1)\,. \tag{2}$$

The maximal width (z_w) is at $\sim 0.5 z_{\max}$.

The flow pattern and the Lorentz factor of the fluid elements are closely related to the distribution of the pressure in the jet through the relativistic Bernoulli's equation $\Gamma\, P^{1/4}$=const., i.e., the flow is faster (slower) where the pressure decreases (increases). The distribution of the flow velocity, Lorentz factor and Doppler beaming factor are, therefore, non-uniform both along and across the jet. The highest velocity occurs in the most rarefied region where the internal pressure is minimal (at z_w and close to the jet axis). The minimal pressure[1] is given by:

$$P_{\min} = P_0[2{R_p}^{1/4} - 1]^4\,. \tag{3}$$

[1] We point out, there is a printing error in the formula (23) of Daly & Marscher: the power index on the right side should be 4, not $\frac{1}{4}$.

Correspondingly, The maximal Lorentz factor is:

$$\Gamma_{\max} = \Gamma_0/(2{R_p}^{1/4} - 1)\,. \tag{4}$$

The Lorentz factor of the fluid elements along the boundary of the jet is constant:

$$\Gamma_b = \Gamma_0 {R_p}^{-1/4}\,. \tag{5}$$

If the pressure ratio $R_p < 0.5$, shocks will be formed within the jet, leading to electron acceleration and magnetic field amplification etc. In this case the structure and the flow pattern of the jet are much more complicated, but the gasdynamical model of Daly & Marscher (1988) may be still useful to provide a qualitative description for the relativistic jets observed in AGNs. Their analytic expressions may be used to estimate some physical parameters of the jets which are observed to have oscillating structures.

4 A STRATIFIED JET MODEL

Before making a specific model to explain the phenomenon observed in 3C 273 (i.e., the spectral reversal and its correlation with the transverse expansion of the jet), we show some observational evidence for transverse structure (or stratification) in extragalactic jets.

As Krichbaum et al. (2001) pointed out, for 3C 273, a comparison between the 86 GHz VLBI maps of 3C 273 and its quasi-simultaneous 15–22 GHz maps shows that the emission is more concentrated to the jet axis at 86 GHz than at the lower frequencies. This phenomenon is also observed in other AGNs, for example in 3C 454.3 (Krichbaum et al. 1998b; Pauliny-Toth 1998). Similarly, such a difference in the transverse distribution of radiation has also been observed between the optical and radio emissions in several extragalactic jets. The best example is M 87. Its optical jet is observed significantly narrower than the radio jet, i.e., the optical emission is concentrated much more closely to the jet axis than the radio emission (Biretta 1996; Owen et al. 1989; Sparks et al. 1994; Perlman et al. 1999). Therefore there is quite strong observational evidence for the transverse stratification of radiation in extragalactic jets. This might be due to concentration of higher energy electrons or stronger magnetic fields closer to the jet axis.

Combining the radiation stratification with the transverse gradients of the flow properties across the jet described in the last section, we would come to the conclusion that the spectral reversal observed in 3C 273 may be related to the transverse stratification of the physical parameters of the jet (flow velocity, electron density, electron energy and magnetic field, etc.).

4.1 Description of the Model

In fact, as it can be seen from Fig. 2, the spectral reversal of the superluminal knot C12a at epoch 1995.15 is mainly caused by the dramatic increase of its 86 GHz flux density. Relative to epoch 1994.0 the 86 GHz flux density at 1995.15 increased by a factor of ~ 6. At the same time the flux density at 22 GHz increased only by a factor of ~ 2. This differential increase of flux density at the two frequencies may imply that the 86 and 22 GHz emissions are produced in different regions. In the following we consider a simplified model (see Fig. 3): an emitting plane (for example a plane shock) propagates along the jet and its inner part close to the jet axis and designated as component A, has different emission properties from the outer part (component B). Since the spectral reversal of the knot C12a occurred within the period from $\sim$1994.0 to 1995.2 and the spectral index at $\sim$1996.1 had already recovered to its previous value, we assume that this phenomenon was occurring when the emitting region propagated within one oscillation

wavelength. In addition, we assume that component A radiates most of the 86 GHz emission and component B radiates most of the 22 GHz emission.

According to Daly-Marscher's model the two components are assumed to have different flow Lorentz factors, because the inner component A moves through a more rarefied region.

4.2 Geometry and Parameters

Since the concrete processes which cause the spectral reversal could not be specifically defined, our main attempt is to choose some appropriate parameters for the jet flow and the two components to make a model fit to the spectral reversal of knot C12a.

As shown in Fig. 3, the emitting region is propagating along the Z-aixs from $Z = 0$ to $Z = Z_{\max}$. The maximal jet width is at $Z = Z_w$. Since the spectral reversal is associated with the maximal jet width, we assume that the emitting region was at position Z_w at epoch 1995.15. We specifically choose the following values:

$r_0 = 0.35$ mas, $\Gamma_0 = 3.0$ and $R_p = 0.30$.

Then, using the formulae given in section 3 we obtain:

$z_{\max} = 12.0$ mas, $r_{\max} = 0.69$ mas,

$\Gamma_{\max} = 6.3$ and Γ_b=4.1.

Taking the angle between the jet axis and the observer to be θ=10°, we have the projected (or observed) oscillation wavelength $\lambda_{\rm obs} = Z_{\max}\ \sin\theta$=2.08 mas. Thus, as seen from Fig. 1, the emitting region (C12a) was at $Z = 1.04$ mas and $Z = 0.34$ mas for epochs 1995.15 and 1994.0, respectively. The distance separation between the two epochs implies that the average apparent velocity of C12a ia $\sim$0.60 mas yr^{-1} or $\sim 4c$. This is consistent with the VLBI measurements which give (3.9±0.2)c (Krichbaum et al. 2001). The other values chosen for r_0, $r_{\max}$ and $\lambda_{\rm obs}$ are also consistent with the VLBI measurements of the jet width and oscillating wavelength.

4.3 Parameters for Emitting Components

In order to explain the observed spectral reversal of knot C12a, we need to give the relevant parameters for the emitting region. As argued above, the emitting region is assumed to consist of two parts: an inner part (component A) and an outer part (component B). We assume that these two components are homogeneous synchrotron sources, but they produce different synchrotron spectra. In order to choose appropriate parameters for the two components and to construct theoretical spectra to fit those observed at epochs 1994.0 and 1995.15, we assume that the electron energy has a power-law distribution in the comoving frame: $N_*(E_*)$=$N_{0*}{E_*}^{-s}$ with $s = 2.5$ (optically thin spectral index α=0.75). The specific set of parameters chosen for the model fit is shown in Table 1.

Table 1 Parameters for the Stratified Jet Model

	epoch 1994.0		epoch 1995.15	
	component A	component B	component A	component B
Z (mas)	0.34	0.34	1.04	1.04
r_b (mas)	0.46	0.46	0.69	0.69
r-range	0-0.2r_b	0.2-1.0r_b	0-0.2r_b	0.2-1.0r_b
Γ	3.5	3.0	6.3	4.5
N_{0*} (cgs)	$4\,10^{-3}$	10^{-3}	$3.2\,10^{-3}$	$1.2\,10^{-3}$
B_*(G)	$3.5\,10^{-3}$	$7\,10^{-4}$	$6\,10^{-3}$	$3.5\,10^{-4}$
Δz (mas)	0.015	0.015	0.015	0.015

4.4 Model Fit of Spectral Reversal

Having given the parameters for the two components at epochs 1994.0 1995.15, we can use the following formulae to calculate the model spectra for the superluminal knot C12a.

$$\kappa_{\nu_*} = c_6(s) N_* {B_*}^{\frac{s+2}{2}} \left(\frac{\nu_*}{2c_1}\right)^{-\frac{s+4}{2}}, \tag{6}$$

$$\tau_{\nu_*} = \frac{\pi}{2} \kappa_{\nu_*} r/\delta \sin\theta\,, \tag{7}$$

$$S(\nu_*) = \frac{c_5(s)}{c_6(s)} {B_*}^{-\frac{1}{2}} \left(\frac{\nu_*}{2c_1}\right)^{\frac{5}{2}}, \tag{8}$$

$$F(\nu) = \left(\frac{\delta}{1+z}\right)^3 \frac{2r\Delta z}{{d_a}^2} S(\nu_*)(1 - e^{-\tau_{\nu_*}})\,. \tag{9}$$

Symbol '*' represents the parameters in the comoving frame, ν — observing frequency (ν=$\delta\nu_*$, δ — Doppler factor), c_1, c_5 and c_6 — constants (see Pacholczyk 1970), κ_{ν_*} — absorption coefficient, τ_{ν_*} — optical depth, B_* — magnetic field strength, d_a — distance, Δz — thickness of the components.

The model spectra for the knot C12a at epochs 1994.0 and 1995.15 are shown in Fig. 4. It can be seen that the model spectra fit the observations for both epochs quite well. Figure 4 reveals that the observed spectral reversal is mainly due to the spectrum of the component A moving towards a higher frequency with a higher turnover flux density. In fact, its spectrum turnover (ν_m, S_m) moves from (35 GHz, 0.9 Jy) to (60 GHz, 4 Jy). This is not only caused by the increasing Doppler factor, but also by the electron acceleration and field amplification.

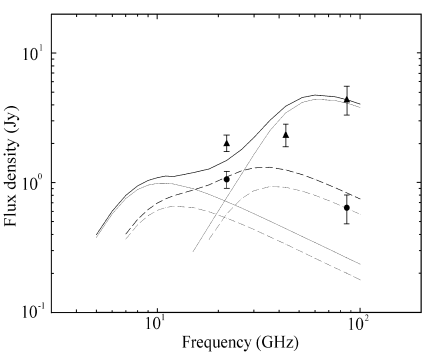

Fig. 4 A model fit for explaining the spectral reversal of the knot C12a. Dashed lines for epoch 1994.0: the spectra of the components (light lines) and the composite spectrum (thick line). Filled points are the observational data, which show the observed spectral index α(22–86 GHz)<0. Solid lines for epoch 1995.15: the spectra of the components (light lines) and the composite spectrum (thick line). Filled triangles are the observational data points, which show α(22–86 GHz)>0.

5 DISCUSSION

On the basis of the concepts on the transverse stratification of the jet, the model proposed in the last section, though oversimplified, can explain the observed spectral reversal of the knot C12a quite well. We should emphasize that, the stratification (or the distributions of the physical parameters across the jet) includes the flow velocity, Doppler beaming, electron density, electron energy, electron acceleration, magnetic field strength and field amplification etc. From the model fit (Table 1) it can be seen that the magnetic field in the component A is much higher than in the component B, i.e., the magnetic field rapidly decreases away from the jet axis. Another characteristic of the model is that effective electron acceleration and field amplification are required. These processes are essential for understanding the jet physics. Future higher resolution mm-cm VLBI observations are desirable to determine the transverse

structure and the distributions of the spectral index and flow velocity both across and along the jet.

The present model is based on gasdynamic properties of relativistic jets. Another possibility for the correlation of the spectral reversal with the jet expansion is Kelvin-Helmholtz instability. Investigation of stratification of jets through the K-H instability is desirable.

Acknowledgements SJQ acknowledges the support from the Max-Planck-Institut für Radioastronomie during his visit (1999–2000).

References

Abraham Z., Carrara E. A., Zensus J. A. et al., 1996, A&AS, 115, 543
Abraham Z., Romero G. E., 1999, A&A, 344, 61
Bååth L. B., Padin S., Woody D. et al., 1991, A&AS, 241, L1
Babadzhanyants M. K., Belokon E. T., 1992, In: E. Valtaoja, M. Valtonen, eds., Variabilty of Blazars, Cambridge University: Cambridge, p.384
Biretta J. A., 1996, In: P. E. Hardee, A. H. Bridle, J. A. Zensus, eds., Energy Transport in Galactic and Extragalactic Jets, ASP Conf. Ser. Vol. 100, San francisco: ASP, p.187
Camenzind M., Kronkenburger M., 1992, A&A, 255, 59
Cohen M. H. et al., 1987, ApJ, 315, L89
Courvoisier T. J. L., Robson E. I., Blecha A. et al., 1988, Nature, 335, 330
Courvoisier T. J. L., 1998, A&AR, 9, 1
Daly R. A., Marscher A. P., 1988, ApJ, 334, 539
Hardee P. E., Clarke D. A., Howell D. A., 1995, ApJ, 441, 644
Krichbaum T. P., Booth R. S., Kus A. J. et al., 1990, A&A, 237, 3
Krichbaum T. P., Witzel A., Graham D. A. et al., 1992, A&A, 260, 33
Krichbaum T. P., Graham D. A., Lobanov A. P. et al., 2001, preprint (MPIfR)
Krichbaum T. P., Alef W., Witzel A. et al., 1998a, A&A, 329,873
Krichbaum T. P. et al., 1998b, In: J. A. Zensus, G. B. Taylor, J. M. Wrobel, eds., Radio Emission from Galactic and Extragalactic Compact Sources, (IAU Colloq. No. 164), ASP Conf. Ser. Vol. 144, p.37
Owen F. N., Hardee P. E., Cornwell T. J., 1989, ApJ, 340, 698
Pacholczyk A. G., 1970, Radio Astrophysics, San Francisco: Freeman,
Pauliny-Toth I. I. K., Porcas R. W., Zensus J. A. et al., 1987, Nature, 328, 778
Pauliny-Toth I. I. K., 1998, In: J. A. Zensus, G. B. Taylor, J. M. Wrobel, eds., Radio Emission from Galactic and Extragalactic Compact Sources, IAU Colloq. No. 164, ASP Conf. Ser. Vol. 144, p.75
Perlman E. S., Biretta J. A., Zhou F. et al., 1999, AJ, 117, 2185
Qian S. J., Witzel A., Krichbaum T. P. et al., 1991, Acta Astron. Sin., 32, 369 (Transl.: Chin. Astron. 1992, 16, 137)
Qian S. J., Krichbaum T. P., Zensus J. A. et al., 1996, A&A, 308, 395
Qian S. J., 1999a, Acta Astrophy. Sin., 19, 8. (Transl.: Chin. Astron., 1999, 23, 166)
Qian S. J., Witzel A., Krichbaum T. P. et al., 1999b, In: L. O. Takalo, A. Sillanpää, BL Lac Phenomenon, ASP Conf. Ser. 159, San Francisco: ASP, p.443
Qian S. J., Zhang X. Z., Krichbaum T. P. et al., 2001, CJAA, 3, 236
Sparks W. B., Biretta J. A., Macchetto F., 1994, ApJS, 90, 909
Türler M., Courvoisier T. J. L., Platani S., 1999a, A&A, 349, 45
Türler M., Paltani S., Courvoisier T. J.-L. et al., 1999b, A&AS, 134, 89
Stevens J. A., Robson I. A., Gear W. K. et al., 1998, ApJ, 502, 182
Von Montigny C., Aller H., Aller M. et al., 1997, ApJ, 483, 161
Zensus J. A. et al., 1990, AJ, 100, 1777
Zensus J. A., 1997, A&AR, 35, 607